Liquid Fuel Spray Processes in High-Pressure Gas Flow

Robert D. Ingebo
Lewis Research Center
Cleveland, Ohio

NASA

LIQUID FUEL SPRAY PROCESSES IN HIGH-PRESSURE GAS FLOW

Robert D. Ingebo*

Atomization of single liquid jets injected down-
stream in high-pressure and high-velocity airflow
was investigated to determine the effect of air-
stream pressure on mean drop size as measured
with a scanning radiometer developed at NASA
Lewis Research Center. For aerodynamic-wave
breakup of liquid jets, it was found that mean
drop diameter D_{32} varied with airstream pres-
sure P_a as follows: $D_{32} \propto P_a^{-0.25}$. This
result was compared with the effect of airstream
pressure on drag and heat-transfer coefficients
of accelerating and vaporizing drops.

INTRODUCTION

The fluid mechanics of producing sprays and the aerothermodynamics
of droplet acceleration and vaporization have been receiving con-
siderable attention in spray process research studies. Spray
drying for food processing, spray painting of manufactured items,
pesticide sprays for agricultural use, icing sprays in wind tun-
nels, and fuel sprays in gas turbine combustors are some of the
major fields of application of spray process studies. In the
field of combustion, Ingebo (1) determined that the fuel spray
vaporization rate is very important in determining burning
characteristics such as ignition delay, flame stability, and
completeness of burning. Fuel droplets formed by atomization
simultaneously accelerate and evaporate in airstreams and thereby
produce a combustible fuel-air mixture. Chemical reaction between
fuel and air, or oxidant vapor, produces a combustion gas stream
of relatively high velocity, temperature, and pressure, which
accelerates the drops as the chemical reaction continues to accel-
erate the combustion gas flow in the combustor. Thus, a clear
understanding of liquid fuel spray combustion requires knowledge
of how aerothermodynamics and fluid mechanics may control the
processes of atomization, vaporization, and acceleration, and how
these processes are related to chemical reaction in determining
combustor performance and exhaust emissions. More specifically,
initial drop size and velocity as well as combustion gas condi-
tions must be known to calculate heat-transfer and drag coeffi-
cients and thereby determine the lifetime histories of burning
fuel drops. New data of this type are especially needed to

*National Aeronautics and Space Administration, Lewis Research
Center, Cleveland, Ohio 44135

determine rates of drop vaporization and combustion under high-pressure gas flow conditions.

Empirical expressions are quite useful in the design of fuel injectors for combustor applications since fuel nozzles can be calibrated with water, and mean drop diameters can then be calculated for the desired fuel, such as Jet-A, with the aid of such correlations. The product of the Weber and Reynolds numbers WeRe has been correlated with atomization data, and, for the condition WeRe > 10^6, atomization occurs in the regime of aerodynamic breakup. This condition was chosen for this investigation since the airstream velocity in turbojet combustors at idle, take-off, and cruise operating conditions is usually quite high; i.e., combustor reference velocities are generally of the order of 20 to 30 m/s.

Since previous studies on atomization were limited to atmospheric pressure conditions, the present investigation was made to determine the effect of airstream pressure on mean drop size. Water jets injected downstream were atomized in the airflow, and mean drop diameters were measured with an improved scanning radiometer recently developed at NASA Lewis Research Center. Combustor inlet-air static pressure was varied from 0.10 to 2.10 MPa over a range of airflow rates per unit area of 10 to 177 g/(cm^2)(s) at 293 K. Two injector tubes with orifice diameters of 0.1016 and 0.216 cm, respectively, were used with liquid flow rates of 27 to 68 liters/hr. Mean drop diameter data were correlated with the Weber-Reynolds number WeRe and a pressure sensitive molecular scale dimensionless group $gl/\bar{c}^2$. The resulting empirical relations for liquid jet breakup were compared with expressions obtained in previous experimental investigations. Also, the effect of airstream pressure on atomization is compared with airstream pressure effects on droplet acceleration and vaporization rates as reported in previous spray studies in order to bring together high-pressure airflow data for spray processes reported in the literature.

APPARATUS AND PROCEDURE

The high-pressure airflow apparatus and auxiliary equipment are shown in figure 1. The test section, water spray, and scanning radiometer optical path are shown in figure 2. Two 5.1-cm-diameter windows pass the laser beam through the spray 25.4 cm downstream of the fuel injector. Single jets of water were injected downstream at the duct centerline with the fuel tube shown in figure 2. Two different 0.635-cm-outside-diameter tubes were used to obtain drop size data with two orifice diameters of 0.1016 and 0.216 cm, respectively.

At 273 K, single water jets were injected downstream at flow rates of 27 and 68 liters/hr, respectively, as measured with a turbine flowmeter. After setting water and airflow rates, mean drop diameter data were obtained with the scanning radiometer shown in figure 2. The optical system consisted of a 1-mW helium-neon laser, a 0.003-cm-diameter aperture, a 7.5-cm-diameter collimating lens, a 10-cm-diameter converging lens, a 5-cm-diameter

collecting lens, a scanning disk with a 0.05-cm-diameter hole, a timing light, and a photomultiplier detector.

The spatial resolution of the scanning radiometer is 2.86 cm, which is also the laser beam diameter in the test section where a sufficient volume of spray was sampled to minimize spray pattern effects on mean drop diameter. Also, the effect of drop size distribution function on the scanning radiometer measurements is discussed in detail by Dobbins, et al. (2), who found that the irradiance distribution is only weakly related to the particle diameter distribution function. Thus, irradiance distribution was used in determining Sauter mean diameter, and changes in the drop size distribution function were assumed to have negligible effect on mean drop size correlations. Reproducibility tests showed that experimental measurements of mean drop diameter agreed within +5 percent. Three sets of monosized polystyrene spheres having diameters of 25, 50, and 100 μm, respectively, were used to calibrate the scanning radiometer. A more complete description of it and the method of determining mean particle size are discussed by Buchele (3,4).

EXPERIMENTAL RESULTS

To determine the effect of airstream pressure on liquid jet atomization, an improved model of the scanning radiometer was developed at NASA Lewis Research Center. It was used to measure the mean diameter of droplets in sprays produced by liquid jets breaking up in high-pressure and high-velocity airflow.

Liquid jet atomization

In a previous study conducted with atmospheric pressure airstreams, drop size distribution data for the breakup of liquid jets were obtained with the high-speed droplet tracking camera shown in figure 3 and described by Ingebo and Foster (5). Photomicrographs of the droplets and a schematic of the liquid jet breakup process are shown in figure 4. Short wavelength disturbances near the injector orifice produce relatively small droplets and grow into longer wavelengths as the jet penetrates farther into the airstream and produces relatively large drops. Mean drop size measurements obtained with this imaging technique gave the data shown in figure 5 for five different liquids. The following correlation of the ratio of mean diameter to orifice diameter D_{30}/D_O with the Weber-Reynolds number $WeRe$ was derived for values of $WeRe < 10^6$:

$$D_{30}/D_O = 3.9(WeRe)^{-0.25} \qquad (1)$$

In deriving this relationship in reference (5), the spatial size distribution data obtained with the high-speed camera were mass weighted using the liquid-concentration profile data obtained with a sampling probe. The temporal size distribution produced is more useful in combustion studies.

In a later study, an early model of the scanning radiometer as described by Ingebo (6) was used to study liquid jet breakup. Here it was found that equation (1) was valid only in the regime

3

of capillary-wave breakup which occurs for values of WeRe $< 10^6$.
At values of WeRe $> 10^6$, it was found in reference (6) that

$$D_O/D_{32} = 0.027(WeRe)^{0.4} \qquad (2)$$

for liquid jet atomization in the regime of acceleration-wave
breakup. Date from reference (6) for both capillary and
acceleration-wave breakup are plotted in figure 6.

In this investigation an attempt was made to extend the appli-
cation of equation (2) to the atomization of liquid jets in high-
pressure airflow. Single jets of water were injected axially
downstream in airstreams having static pressures from 0.1 to
2.7 MPa. Atomization data obtained with the two different fuel
injector tubes are shown in figure 7 where the reciprocal mean
drop diameter D_m^{-1} is plotted against airstream mass velocity
$\rho_a V_r$. As shown, the effect of $\rho_a V_r$ on D_m^{-1} decreases mark-
edly as airstream pressure is increased from 0.1 to 2.7 MPa. To
extend equation (2) and make it applicable to high airstream pres-
sures, $(D_O/D_m)(WeRe)^{-0.4}$ is plotted against the pressure sensitive
group $gl/\bar{c}^2$(fig. 8). In this dimensionless group g is the
acceleration due to gravity, l the mean free molecular path,
and $\bar{c}^2$ the root-mean-square velocity of the air molecules.

The evaluation of this dimensionless group is as follows. The
mean free molecular path l may be expressed as

$$l = 1/\sqrt{2}nD_g^2 = 6.11 \times 10^{-6} \text{ cm}$$

since the number of molecules per cubic centimeter n is 2.7×10^{19}
at a temperature of 0 °C and a pressure of 1 atm and the diameter
of an air molecule D_g is 3.7×10^{-8} cm.

The root-mean-square molecular velocity $\bar{c}$ may be expressed as
$\bar{c} = (3RT/M)^{0.5}$, which yields

$$\bar{c}^2 = \frac{(3)(8.31 \times 10^7)(273)}{29} = 2.35 \times 10^9 (\text{cm/s})^2$$

Since g is 980 cm/s/s,

$$gl/\bar{c}^2 = \frac{(980)(6.11 \times 10^{-6})}{2.35 \times 10^9} = 2.55 \times 10^{-12}$$

From the data plotted in figure 8, it is evident that
$D_m^{-1} \sim (gl/\bar{c}^2)^{0.15}$. Thus, the following expression is obtained
from the data plotted in figure 9:

$$D_O/D_{32} = 1.2(WeRe)^{0.4}(gl/\bar{c}^2)^{0.15} \qquad (3)$$

which agrees with the expression obtained by Ingebo (7) for the
cross stream injection of liquid jets - i.e.,

$$D_O/D_{32} = 1.4(WeRe)^{0.4}(gl/\bar{c}^2)^{0.15}$$

for acceleration-wave breakup of liquid jets with values of $WeRe > 10^6$. Since the molecular-scale momentum-transfer group gl/c^2 is inversely proportional to airstream pressure, it is evident that $gl/c^2 \sim P_a^{-1}$. It was just shown that, at 273 K and 1 atm pressure, $gl/c^2 = 2.55 \times 10^{-12}$. Also, since $WeRe \sim P_a$, equation (3) shows that $D_{32} \sim P_a^{-0.25}$. Thus, the effect of airstream pressure on D_{32} is somewhat less than that which would be obtained by extrapolating an atmospheric pressure expression up to high airstream pressures. For example, equation (2) would indicate that $D_{32} \sim P_a^{-0.4}$.

A comparison of the results obtained by several investigators of airstream effects on atomization is given in table I. Best agreement was obtained with Lorenzetto and Lefebvre (8) where it was found that $D_{32} \sim P_a^{-0.3}$. This is in good agreement with equation (3) since it is assumed that $D_m = D_{32}$ for the measurements of D_m made with the improved scanning radiometer in the present study. Kim and Marshall (11) and Wolfe and Andersen (12) give values more in agreement with the theoretically predicted relationship $D_{32} \sim P_a^{-0.67}$ given by Adelberg (13). The atomization data presented in this study and in reference (8) were obtained over a much broader airstream pressure range than that used in references (11) and (12). This indicates a need to improve the theory proposed in reference (13), which does not account for molecular-scale forces such as those given in the group gl/c^2.

Droplet drag coefficients for accelerating sprays

The high-speed droplet tracking camera used to obtain drop size data also gave drop velocity data. Thus, it was possible to determine drag coefficients of drops accelerating in gas streams. In the study described by Ingebo (14), it was found that the drag coefficient C_d could be correlated with Reynolds Re based on drop diameter as follows:

$$C_d = 27Re^{-0.84}$$

at atmospheric pressure.

Studies of propellant atomization and droplet acceleration in the high-pressure rocket combustor shown in figure 10 were made with the droplet tracking camera as described by Ingebo (15). It was found that the drag coefficient based on the mean drop diameter D_{20} could be correlated with the Reynolds number Re and the dimensionless group gl/c^2 as follows:

$$C_d = 0.13Re^{-0.84}(gl/c^2)^{-0.2} \tag{4}$$

where Re is based on the area number mean drop diameter D_{20}. A plot of the data used to derive this expression is shown in figure 11. From equation 4, the effect of airstream pressure on drag coefficient appears to be $C_d \sim P_a^{-0.64}$. As in the study of atomization, the effect of airstream pressure is somewhat less than that predicted from atmospheric pressure studies.

Heat-transfer coefficients for vaporizing drops

In the study of vaporization rates of single drops in atmospheric pressure airstreams, Ingebo (16) found that the Nusselt number Nu could be correlated with the product of the Reynolds and Schmidt numbers $ReSc$ as follows: $Nu = 2 + 0.30(ReSc)^{0.6}$, where $Nu = hD/k_g$, h is the heat-transfer coefficient, D the drop diameter, $Sc = \mu/b_{gw}$, k_g and μ the gas thermal conductivity and viscosity, respectively, and b_{gw} the vapor diffusivity. In a later study by Ingebo (17), at an airstream static pressure range of 0.6 to 2 atm, data for the Nusselt number were obtained as shown in figure 12 and the following expression was derived:

$$Nu = 2 + 2.6 \times 10^{6} [(ReSc)(gl/\bar{c}^{-2})]^{0.6} (k_g/k_v)^{0.5} \tag{5}$$

where k_v is the thermal conductivity of the vapor. Thus, $Nu \sim P_a^{0}$. However, airstream pressure still influenced vaporization rate by its effect on temperature difference across the air-vapor film surrounding the drop.

CONCLUSIONS

As a result of this study and previous spray studies in high-pressure airstreams, graphical or numerical integration methods of calculating spray vaporization rates will not be very useful until more atomization, drag coefficient, and heat-transfer coefficient data are available for very high-pressure airstreams. The effects of airstream pressure on mean drop diameter D_{32}, drag coefficient C_d, and Nusselt number Nu are shown in table II for comparison. Probably the most critical need at present is for high-pressure airstream data on drop size distribution and on mean drop size for spray processes in high-temperature and highly turbulent gas streams. Also, a more fundamental picture of simultaneous heat, momentum, and mass transport properties is needed for a more comprehensive treatment of fuel spray processes and the overall combustion process.

NOMENCLATURE

$b_{g,w}$ = molecular mass diffusivity (g/(cm)(s))

C_d = drag coefficient

$\bar{c}$ = root-mean-square molecular velocity (cm/s)

D = diameter (cm)

D_{32} = Sauter mean diameter, $\sum nD^3 / \sum nD^2$ (cm)

g = acceleration due to gravity (980 cm/s^2)

h = heat-transfer coefficient (g-cal)/(sec)(cm^2)(°C)

k = thermal conductivity (g-cal)/(sec)(cm^2)(°C/cm)

l = mean free molecular path (cm)

M   = molecular weight

Nu = Nusselt number for heat transfer, hD/k

n   = number of molecules per unit volume

P   = static pressure (atm)

R   = universal gas constant (8.31×10^7 ergs/(K)(mole))

Re = Reynolds number based on orifice diameter, D_oV_r/γ_l

Sc = Schmidt number based on mass diffusivity, $\mu/b_{g,w}$

V   = velocity (cm/s)

We = Weber number based on orifice diameter, $D_o\rho_aV_r^2/\sigma$

T   = kinematic viscosity (cm^2/s)

σ = surface tension (dynes/cm)

ρ = density (g/cm^3)

μ = absolute viscosity (g/(cm)(s))

Subscripts:

a   = airstream

g   = gas molecule

l   = liquid

m   = mean

o   = orifice

r   = relative

v   = vapor

REFERENCES

1 Ingebo R D , "Atomizing Characteristics of Swirl Can Combustor Modules with Swirl Blast Fuel Injectors," NASA TM-79297, 1980.

2 Dobbins R A, Crocco L, and Glassman I, AIAA J., 1 (1963) 1882.

3 Buchele D R, "Scanning Radiometer for Measurement of Forward-Scattered Light to Determine Mean Diameter of Spray Particles," NASA TM-X-3454, 1976.

4 Buchele D R, "Particle Sizing by Measurement of Forward-Scattered Light at Two Angles," NASA TP-2156, 1983.

5 Ingebo R D, and Foster H H, "Drop-Size Distribution for Cross-Current Breakup of Liquid Jets in Airstreams," NACA TN-4087, 1957.

6 Ingebo R D, "Capillary and Acceleration Wave Breakup of Liquid Jets in Axial-Flow Airstreams," NASA TP-1791, 1981.

7 Ingebo R D, "Aerodynamic Effect of Combustor Inlet-Air Pressure on Fuel Jet Atomization," NASA TM-83611, 1984.

8 Lorenzetto G E, and Lefebvre A H, AIAA J., 15 (1977) 1006.

9 Nukiyama S, and Tanasawa Y, Japan Society of Mechanical Engineers, Transactions, 5 (1939) 63.

10 Weiss M A, and Worsham C H, ARS J., 29 (1959) 252.

11 Kim K Y, and Marshall W R, AIChE J., 17 (1971) 575.

12 Wolfe H E, and Andersen W H, in "Proceedings of the 5th International Shock Tube Symposium," Naval Ordnance Laboratory, White Oak, MD, 1965, pp. 1145-1169.

13 Adelberg M, AIAA J., 6 (1968) 1143.

14 Ingebo R D, "Drag Coefficients for Droplets and Solid Spheres in Clouds Accelerating in Airstreams," NACA TN-3762, 1956.

15 Ingebo R D, "Vaporization Rates of Ethanol Sprays in a Combustor with Low Frequency Fluctuations of Combustion-gas Pressure," NASA TN-D-1408, 1962.

16 Ingebo R D, "Vaporization Rates and Heat-Transfer Coefficients for Pure Liquid Drops," NACA TN-2368, 1951.

17 Ingebo R D, "STudy of Pressure Effects on Vaporization Rate of Drops in Gas Streams," NACA TN-2850, 1953.

TABLE I. - EXPERIMENTALLY DETERMINED E: 'ONENTS OF

PROPERTIES PROPORTIONAL TO RECIPROCAL MEAN DROP

DIAMETER D_m^{-1} FOR AERODYNAMIC-WAVE BREAKUP

OF LIQUID SHEETS AND JETS

Sources for exponents	Airstream velocity, V_a, cm/s	Orifice diameter, D_o, cm	Airstream pressure, P_a, MPa
Experimental (eq. (3))	1.2	0.20	0.25
Nukiyama and Tanasawa (9)	1.0	.00	0
Weiss and Worsham (10)	1.33	-.16	(a)
Kim and Marshall (11)	1.14	.00	.57
Wolfe and Andersen (12)	1.33	b-.17	.67
Lorenzetto and Lefebvre (8)	1.0	0	.30

aUsed variable $1 + \rho_a/\rho_l$.
bExponent for initial drop diameter instead of orifice diameter.

TABLE II. - COMPARISON OF EFFECT OF AIRSTREAM

PRESSURE P_a ON SPRAY PROCESS PARAMETERS

D_m and C_d AND NUSSELT NUMBER Nu

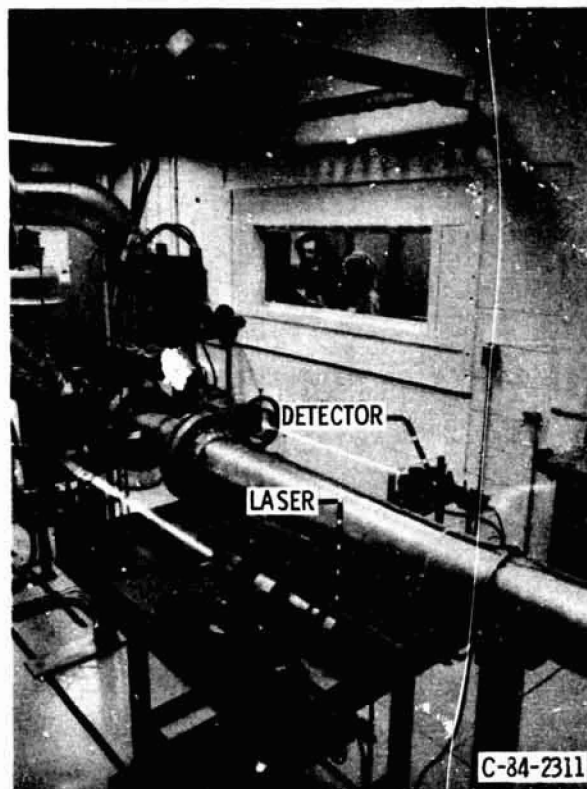| Atomization	$D_o/D_m = 1.2(WeRe)^{0.4}(gl/\bar{c}^2)^{0.15}$ $D_m \sim P_a^{-0.25}$
Acceleration	$C_d = 0.23Re^{-0.84}(gl/\bar{c}^2)^{-0.2}$ $C_d \sim P_a^{-0.64}$
Vaporization	$Nu = 2 + 2.6 \times 10^6[(ReSc)(gl/\bar{c}^2)]^{0.6}$ $h \sim P_a^0$

Figure 1. - Apparatus and auxilliary equipment.

AIR

15.2 cm

7.6 cm

WATER →

LIGHT SCATTERING
ANGLE, 0.05 rad

10 cm

SPRAY

10 cm diam
SCANNER

5 cm diam

FILTER

0.003 cm diam

7.5 cm diam

1-mW
LASER

PHOTO-
MULTIPLIER

TIMER
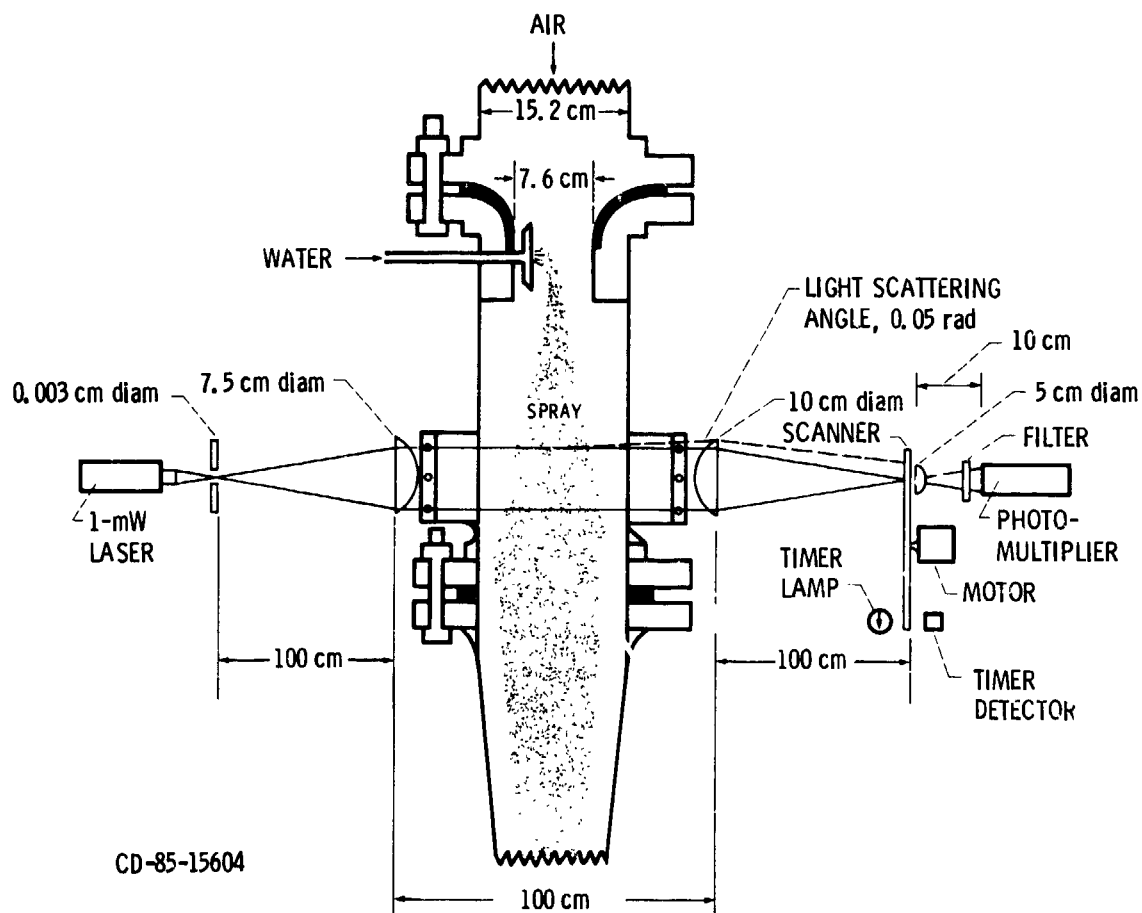LAMP

MOTOR

100 cm

100 cm

TIMER
DETECTOR

CD-85-15604

100 cm

Figure 2. - High-pressure test section and scanning radiometer optical path.

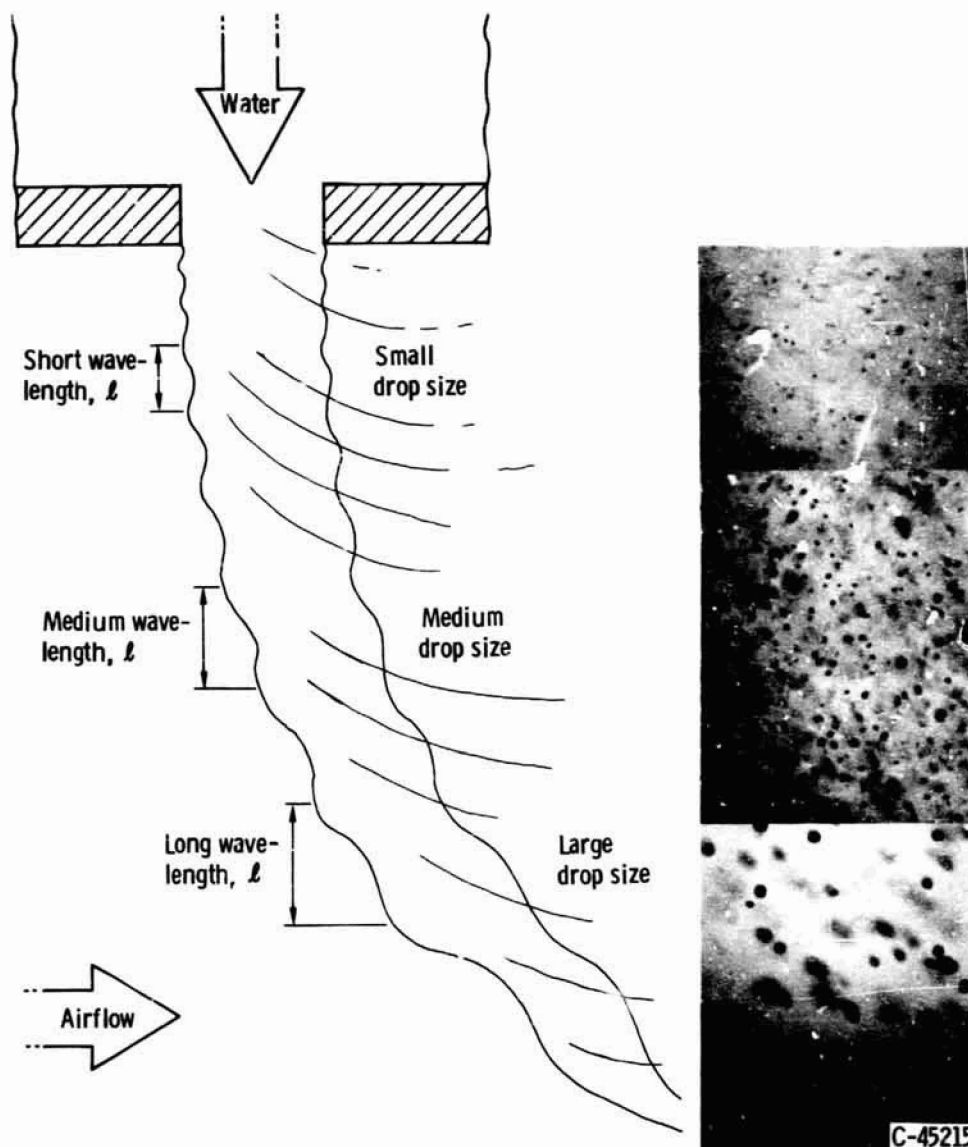Figure 3. - Diagram of test section equipment and camera unit.

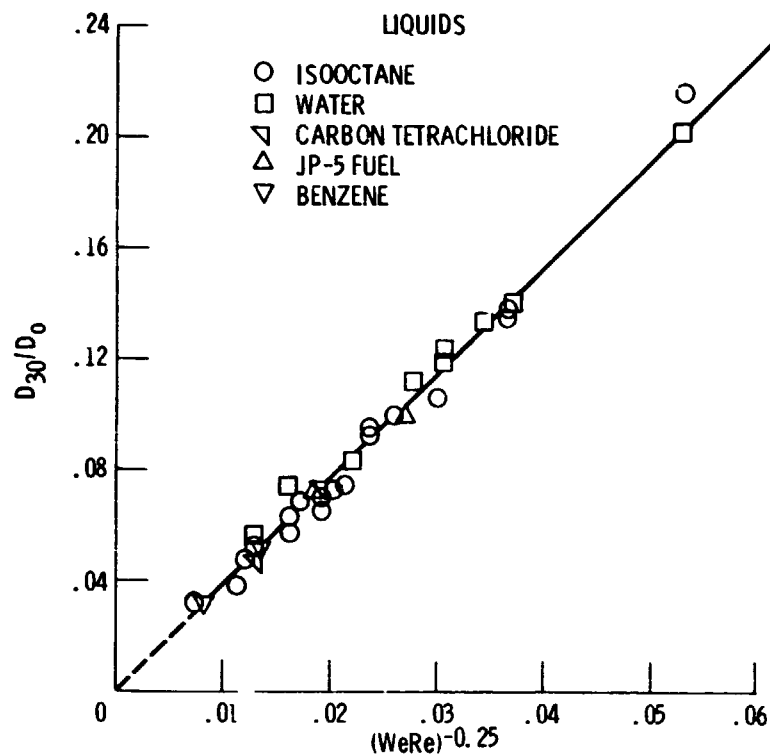Figure 4. - Schematic of a liquid jet breaking up into ligaments and drops with cross-stream injection.

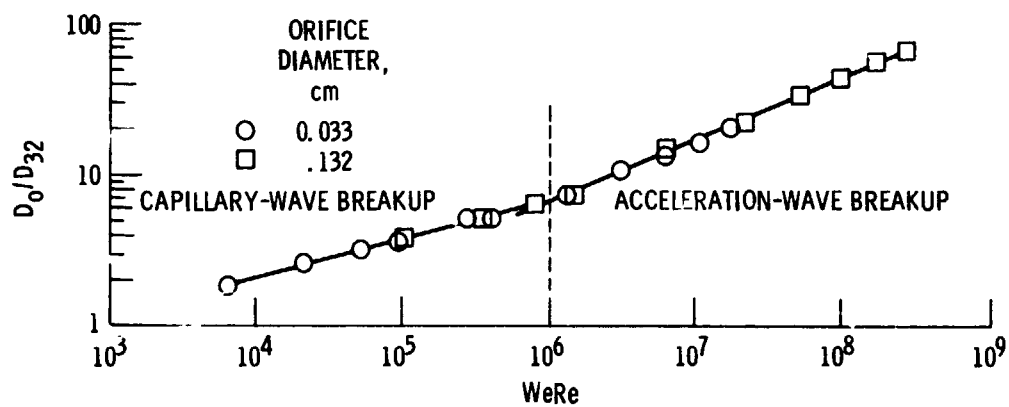Figure 5. - Relation between mean to orifice diameter ratio and Weber-Reynolds number ratio.

Figure 6. - Relation between orifice to mean diameter ratio and Weber-Reynolds number.
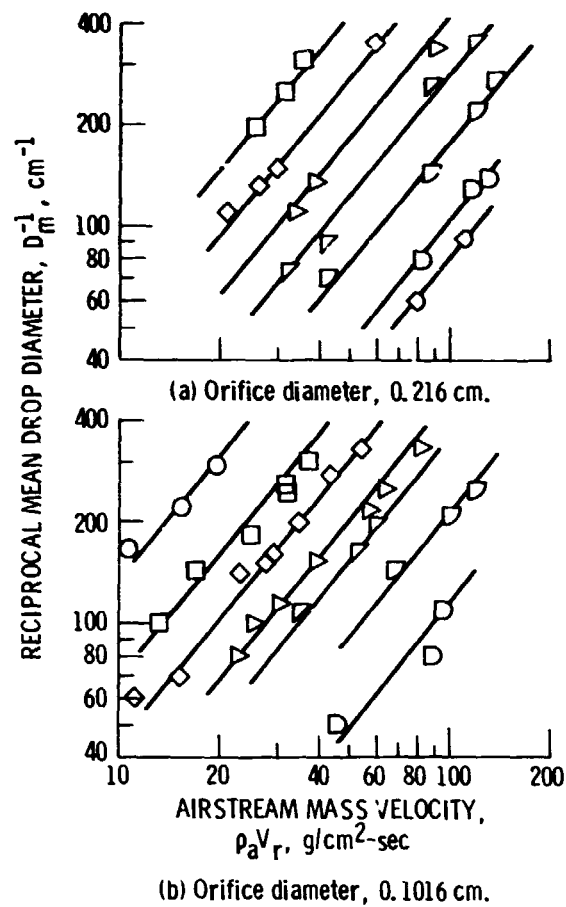
(a) Orifice diameter, 0.216 cm.

(b) Orifice diameter, 0.1016 cm.

Figure 7. - Variation of reciprocal mean drop diameter with airstream mass velocity.

INLET-AIR
STATIC
PRESSURE,
MPa

○	0.10
□	.20
◇	.30
▷	.50
▽	.70
◁	1.10
◻	2.10
◇	2.77

(a) Orifice diameter, D_0, 0.216 cm.

$(D_0/D_m)(WeRe)^{-0.4}$

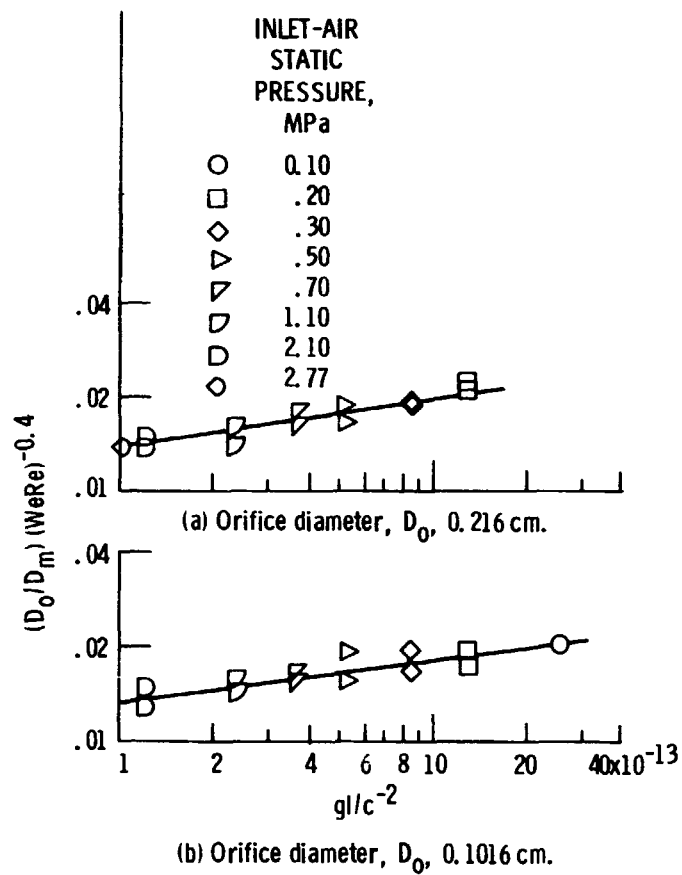(b) Orifice diameter, D_0, 0.1016 cm.

gl/c^{-2}

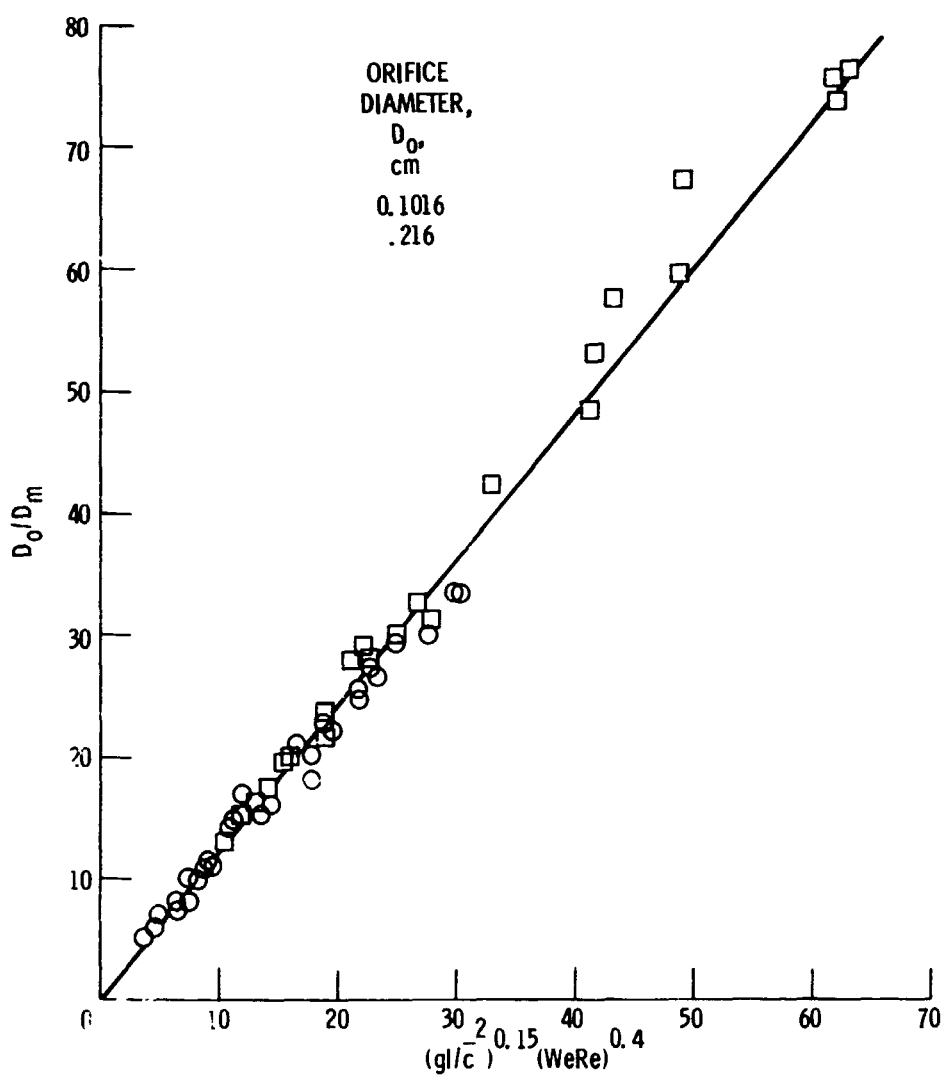Figure 8. – Correlation of mean drop diameter D_m with airstream pressure sensitive group gl/c^{-2}.

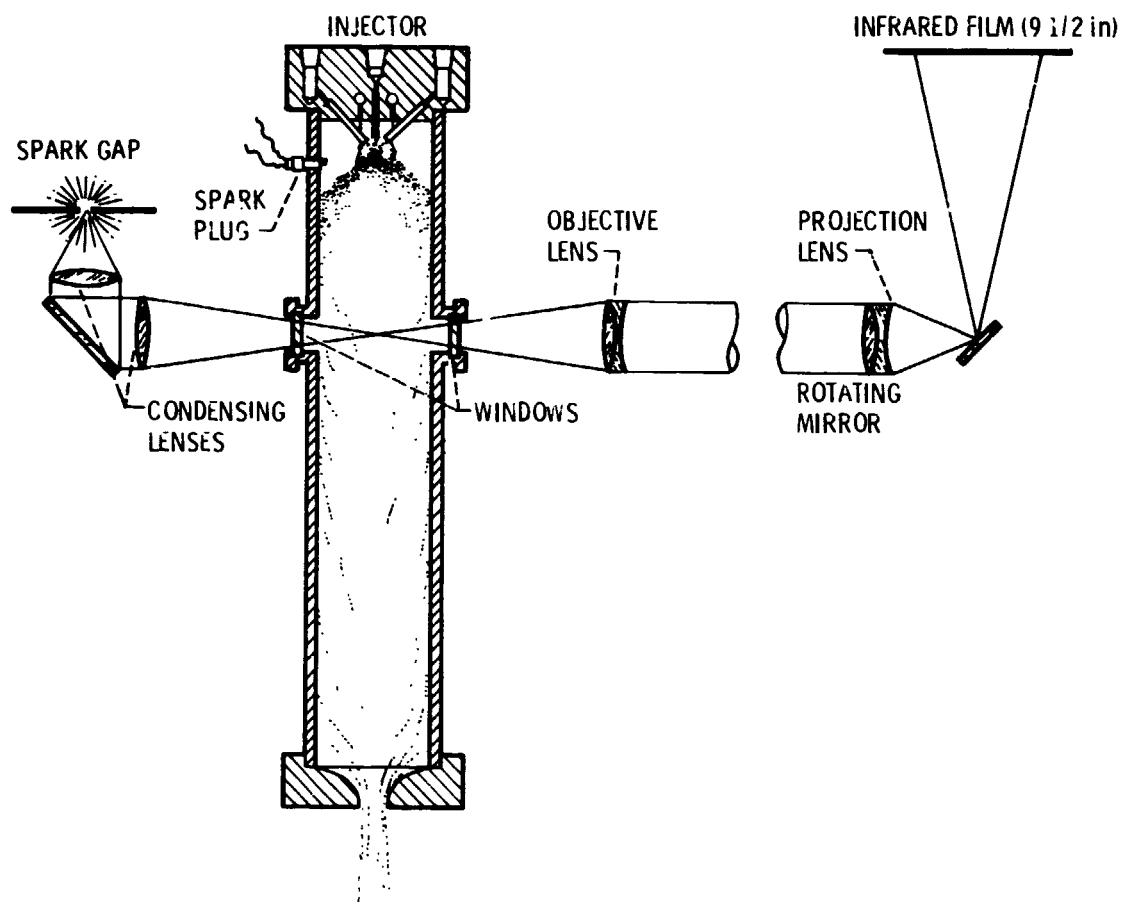Figure 9. - Correlation of mean drop diameter D_m with dimensionless groups $gl/\bar{c}^2$ and WeRe.

Figure 10. – Diagram of experimental apparatus.

FUEL SPRAY　　　　　　　EVALUATION TEMPERATURE AT --

FINE	COARSE	EXPERIMENTAL NUSSELT NUMBER, Nu_{20}	EXPERIMENTAL REYNOLDS NUMBER, Re_{20}	TOTAL HEAT REQUIREMENT PER UNIT OF MASS, H_T, g-cal/g
□	○	T_f	$T = (T_g + T_s)/2$	T_f
◇	□	T_{stoic}	$T'_f = (T_{stoic} + T_x)/2$	T'_f
	△	T_{stoic}	$T'_f = (T_{stoic} + T_x)/2$	T'_f

$$(C_D)_{20} = 0.13\, Re_{20}^{-0.84} (gl/c)^{-0.2}$$

DRAG COEFFICIENT, $(C_D)_{20}$

1.6

1.4

1.2

1.0

.8

.6

.4

.2

2　　4　　6　　8　　10　　12
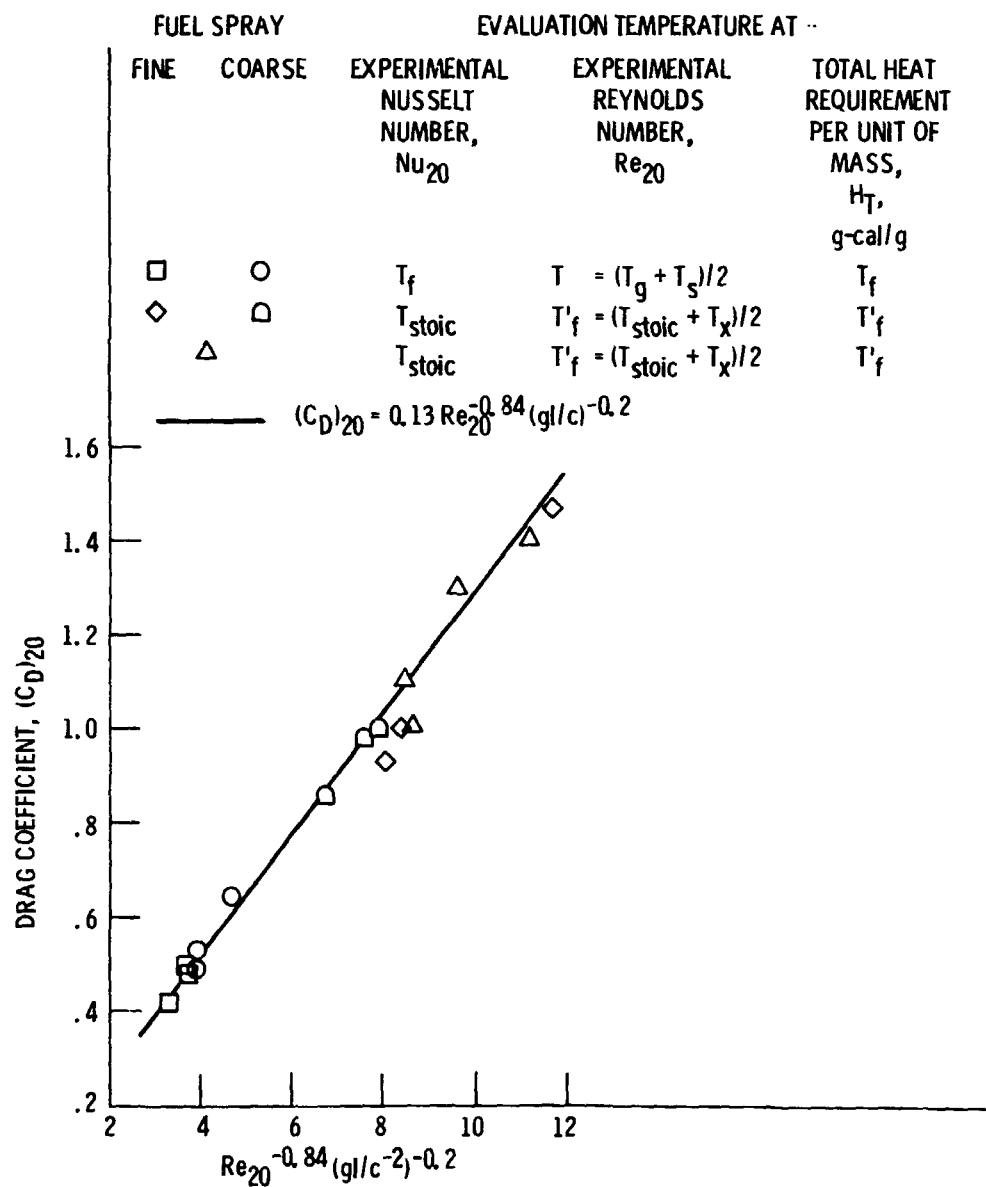
$Re_{20}^{-0.84} (gl/c^{-2})^{-0.2}$

Figure 11. - Correlation of drag coefficient
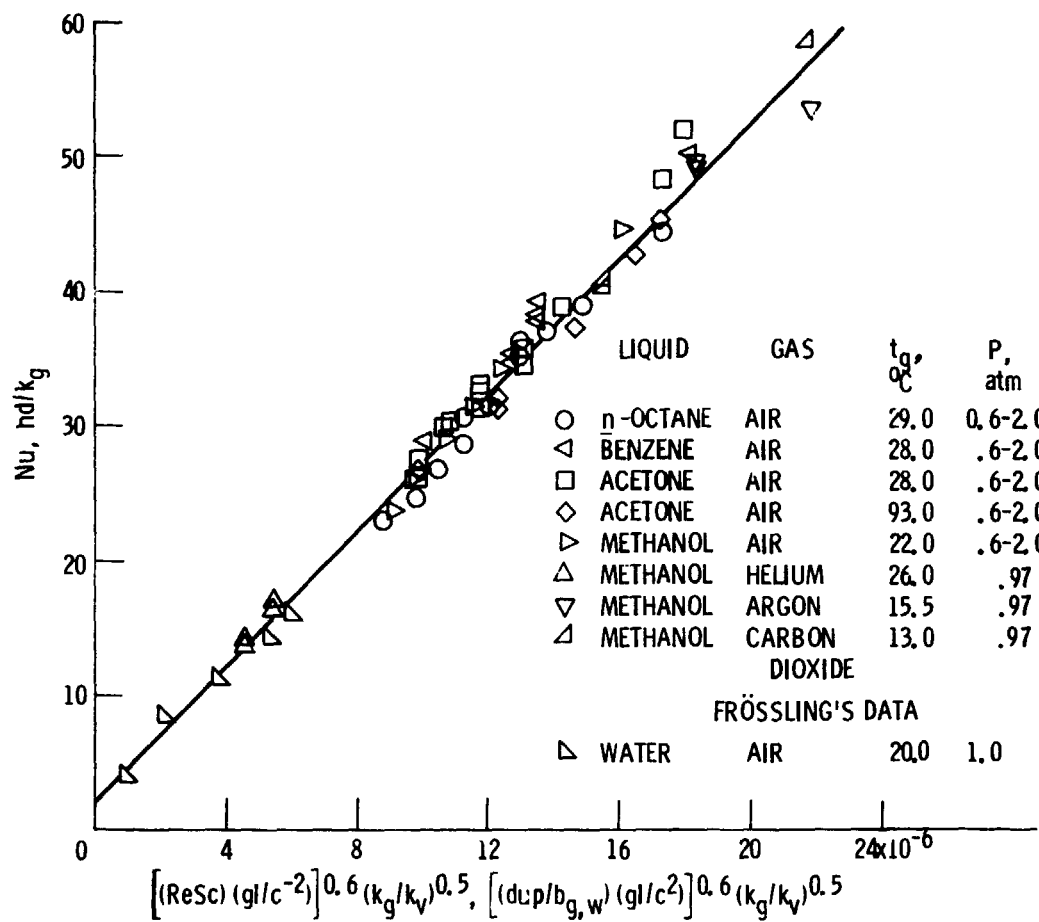with Reynolds number and gl/c^{-2} group.

Figure 12. - Correlation of Nusselt number with momentum-transfer groups and thermal-conductivity ratio.